ELSEVIER

Nuclear Instruments and Methods in Physics Research A 475 (2001) 348–352

NUCLEAR INSTRUMENTS & METHODS IN PHYSICS RESEARCH Section A

www.elsevier.com/locate/nima

Observation of longitudinal phase space fragmentation at the TESLA test facility free-electron laser

M. Hüning, Ph. Piot*, H. Schlarb

Deutsches Elektronen-synchrotron, DESY, D-22603 Hamburg, Germany

Abstract

It has been reproducibly observed that the energy distribution of the beam, when fully longitudinally compressed for SASE operation, breaks up into several peaks. In this paper a description of the experimental setup, beam operating conditions, and observations is presented to enable further theoretical studies of this effect. © 2001 Elsevier Science B.V. All rights reserved.

PACS: 29.27.Bd; 41.20.Bt; 41.60.Ap; 41.85.Lc

Keywords: Bunch compression; FELs; Microbunch; Collective effect

1. Introduction

High-gain single pass free-electrons lasers (FEL) require high charge (nC-level), ultrashort (ps-level) and low emittance (mm-mrd) electron bunches. Since state-of-art photoinjectors cannot directly produce the required short bunch, magnetic bunch compressors are generally used to achieve the picosecond-level bunch length needed. Compressing and then transporting these short bunches to the undulator section becomes challenging since significant phase space dilution due to collective effects (e.g. wakefields, coherent synchrotron radiation, etc) might arise. In this paper, we present a series of measurements taken at the TESLA Test Facility (TTF) FEL [1]. Our observations indicate that a bunch undergoing compression tends to have its energy profile fragmented. It is worthwhile mentioning that similar features have been recently observed at other facilities [2,3].

2. Experimental background

A schematics of the TTF FEL driver accelerator is depicted in Fig. 1. We will only concentrate on the longitudinal phase space manipulation since the measurements reported hereafter pertain to this plane. The beam generation line consists of a L-band radio-frequency (RF) photoinjector coupled to a TESLA-type superconducting accelerating cavity that boosts the beam up to 17 MeV. The photocathode drive-laser is Gaussian-shaped with a rms time duration of 8 ps. The electron bunch then enters an accelerating section (Acc. #1) that consists of eight TESLA-type superconducting cavities. The injection phase of the beam in this latter accelerating section is chosen, under nominal

*Corresponding author. Tel.: +49-0-40-8998-2755.
E-mail address: philippe.piot@desy.de (P. Piot).

0168-9002/01/$ - see front matter © 2001 Elsevier Science B.V. All rights reserved.
PII: S0168-9002(01)01537-6

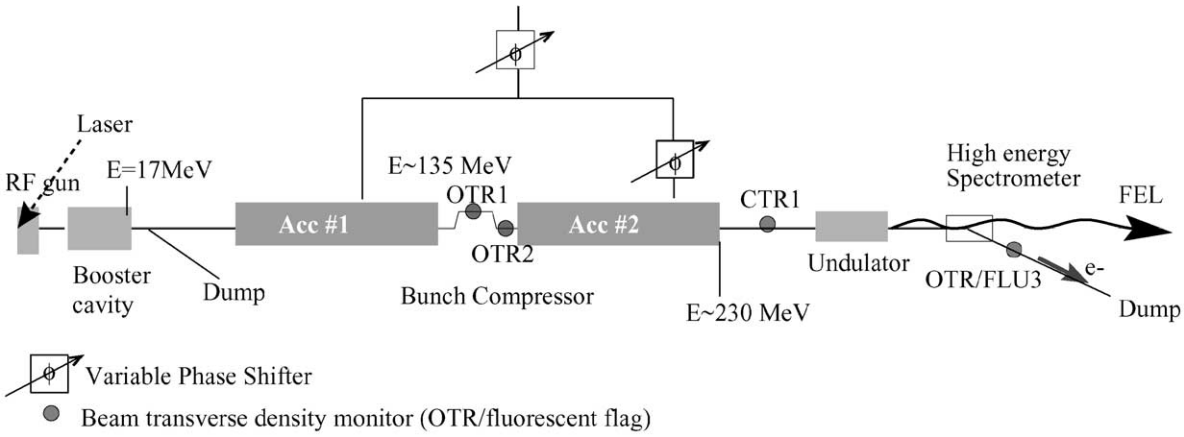


Fig. 1. Overview of the Tesla Test Facility phase I.

operating conditions, to impart the proper time–energy correlation to compress the bunch using the downstream magnetic chicane-based compressor. The beam transport downstream of the bunch compressor consists of a second accelerating section (Acc. #2, identical to Acc. # 1), nominally operated for maximum energy gain, followed by an undulator. Behind the undulator, the electron beam is separated from the FEL beam by a spectrometer dipole (that bends in the same plane as the compressor). The transfer line to the dump is instrumented with several diagnostics including a beam profile measurement station.

A detailed description of the magnetic compressor is presented in Ref. [4]. During our measurement, the bending angle in the compressor was set to 19°, which corresponds to a momentum compaction $R_{56} \simeq -0.18\,\mathrm{m}$. This results in an optimum operating phase for the first accelerating section of 10° off-crest approximately. Because of the rather long bunch length at the injector front-end, typically 2.7 mm (rms), the longitudinal phase space is strongly distorted via RF-induced curvature during its acceleration in Acc. #1. This distortion affects the compression process and limits the minimum attainable bunch length to 0.5 mm (rms) approximately (as inferred from multi-particle simulations and experimentally verified).

3. Experimental techniques

During our measurements, we used the different beam profile monitors showed in Fig. 1: the energy spread was measured using the optical transition radiation (OTR) viewers OTR1 and OTR/FLU3 (this latter viewer incorporates both an OTR radiator and a fluorescent screen). At the location of these two beam profile stations, the linear dispersion is estimated to $R_{16} = 0.31\,\mathrm{m}$ (bunch compressor) and $R_{16} = -1.15\,\mathrm{m}$ (spectrometer), respectively. The nonlinear dispersion, T_{166}, is found, for both locations, to have insignificant impact on the beam horizontal profile so that the horizontal coordinate of an electron, x, scales linearly (to first order) with its relative momentum offset, δ, following $x \simeq R_{16}\delta$. This scaling implicitly assumes that the contribution from the pure betatron term is insignificant. A true assumption since, for all measurements presented in this paper, a set of quadrupoles, located upstream of the bunch compressor or the spectrometer dipole, respectively, were tuned to minimize the horizontal beam spot at the observation point. This guarantee that the beam spot was dominated by the dispersive contribution. Based on the measurements of energy profiles at OTR/FLU3 for different phases of Acc. #2, a longitudinal tomography technique was implemented. The method to reconstruct the longitudinal phase space is

based on the MENT [5] (Maximum ENTropy) algorithm which computes the best estimate of the phase space density by maximizing its entropy. At the compressor exit the transverse beam density can also be measured using OTR2. At that point the dispersion was found not to be zero, we believe because of spurious dispersion generated by nonzero value of upstream correctors. The diagnostics package also include a bunch length monitor located downstream of the second accelerating section. This device provides bunch length measurement by the mean of a sub-millimeter wave polarizing interferometry of coherent transition radiation [6] (CTR). We did not systematically measure the bunch length but rather inferred whether the first accelerating section (Acc. #1) was operated for maximum compression by simply "peaking" the CTR power detected by a pyroelectric detector. All of the measurements reported in the following were performed with a charge per bunch of 1 nC (within 10%). We have verified, using a streak camera setup, that our observations result from a single RF-bucket.

4. Observations

4.1. Energy profiles versus incoming time-energy correlation

In this series of measurement the compressor is operated, and the bunch compression is varied by operating Acc. #1 at different phase to act on the incoming longitudinal phase space slope, $d\delta/ds$: at maximum compression it is related to the bunch compressor momentum compaction by relation $d\delta/ds = -1/R_{56}$. We found, using the CTR signal, that the maximum compression was occuring -10° w.r.t. the maximum energy gain phase. For this operating condition, the beam energy was about 135 MeV at the bunch compressor location and 230 MeV downstream Acc. #2. After each change of Acc. #1 phase, the phase of the Acc. #2 accelerating section was reset to maximize the energy at the machine front end. Fig. 2 depicts the evolution of the beam density recorded at the observation point (i.e. OTR/FLU3) for some phase of the Acc. #1. The maximum compression

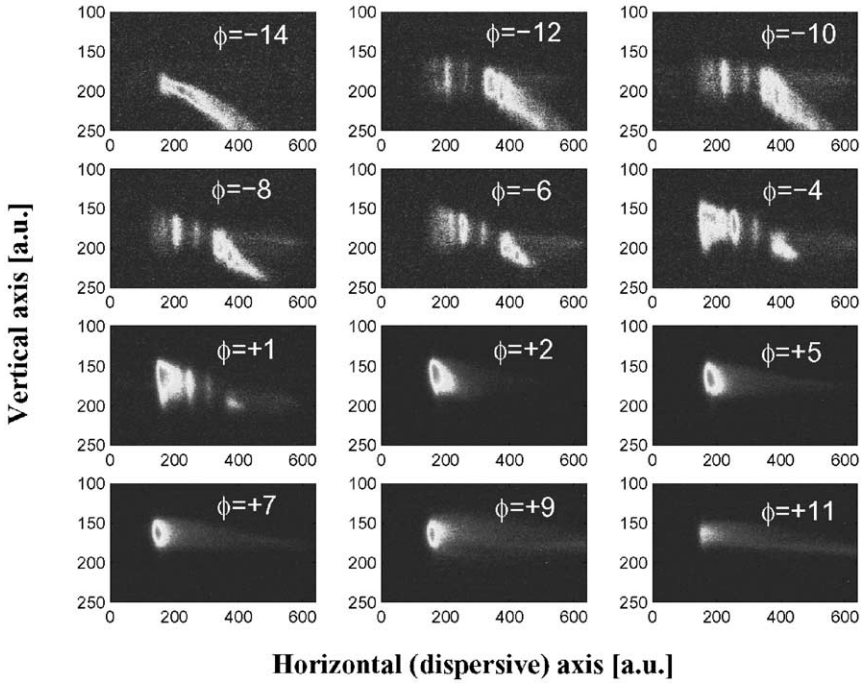


Fig. 2. Single bunch beam transverse density observed at the profile measurement station OTR/FLU3. These measurements were performed using the fluorescent screen.

occurs at $\phi \simeq -8°$[1] whereas the maximum energy gain through the whole linac is obtained for $\phi \simeq +2°$, From Fig. 2, we conclude that when the time–energy-induced correlation by Acc. #1 does not provide compression, i.e. $\phi > +2°$, the energy profile is as expected: it consists of a bright core with a long energy tail due to the RF-induced curvature because of the long incoming bunch. As the time–energy-induced correlation allows compression, $\phi < +2°$, the energy profile multiple fine structure which seems to separate into two main "islands" at maximum compression. Finally, in the over-compression regime, $\phi < -8°$, these multiple structures start disappearing and are hardly observable at phases below $-14°$.

4.2. Impact of the bunch compressor

For three cases (i) bunch compressor operated and accelerated section Acc. #1 operated for maximum compression, (ii) bunch compressor operated and Acc. #1 operated on-crest, and (iii) bunch compressor off with Acc. #1 operated approximately $-10°$ off-crest, we have investigated the evolution of the energy profile in the high energy spectrometer line for various phase of Acc. #2 ultimately to take tomographic data in order to recover the full longitudinal phase space density. The energy profiles for these three cases are presented in Fig. 3 (Acc. #2 was set for maximum energy gain). A structured energy profile, as the one presented previously, is observed only for the case where the linac operated to provide maximum compression. This feature, which has also been observed for other bunch charges, suggests the induced fragmentation of the energy profile related to the compression process. At the bunch compressor exit, some structure can already be noticed by observing the beam transverse density at OTR2, but none was observable at OTR1. For case (ii), the reconstructed longitudinal phase space at the compressor exit is shown in Fig. 4.

[1] The phase value ϕ mentioned hereafter are arbitrary value read from the control system

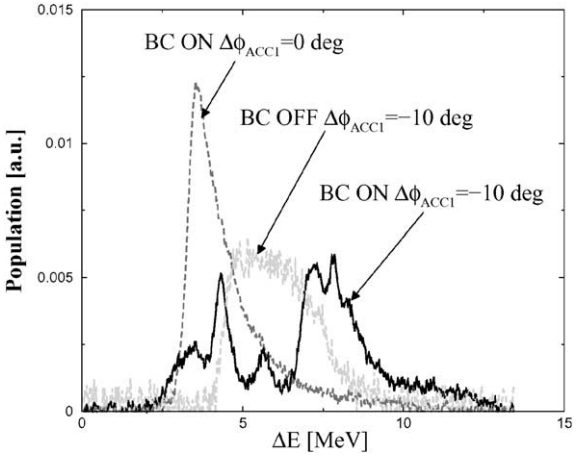


Fig. 3. Energy profile obtained for three different senarii of operation: bunch compressor ON with Acc. #1 on-crest ($\Delta\phi = 0°$), and the setup for minimum bunch length ($\Delta\phi = 0°$), and bunch compressor OFF with $\Delta\phi = -10°$.

4.3. Charge-dependence

To check whether the observation could be attributed to collective effects, we also measured the energy distribution for bunch charge ranging from 0.5 to 4 nC. The energy profile showed a weak dependence on the charge. Nevertheless the collective effects[2] hypothesis cannot be ruled out: the charge was varied by changing the photocathode drive laser intensity, which also impacts the bunch length. From multi-particle simulations we expect that increasing the charge from 0.5 to 4 nC would approximately double the bunch length (from 2 to 4 mm (rms)) principally because of longitudinal space charge force charge-dependence in the RF-gun and following drift section.

5. Discussion

An anomalous "beam break-up" of the longitudinal phase space has been observed at TTF-

[2] for the collective effects considered, the relative energy loss of one electron is of the form $\delta p/p \propto Q/\sigma_s^{\alpha}$, for standard geometric wakefield $\alpha \simeq \frac{1}{2}$, for coherent synchrotron radiation $\alpha = \frac{4}{3}$, with Q being the bunch charge. The charge density is assumed to be a Gaussian distribution with rms length σ_s.

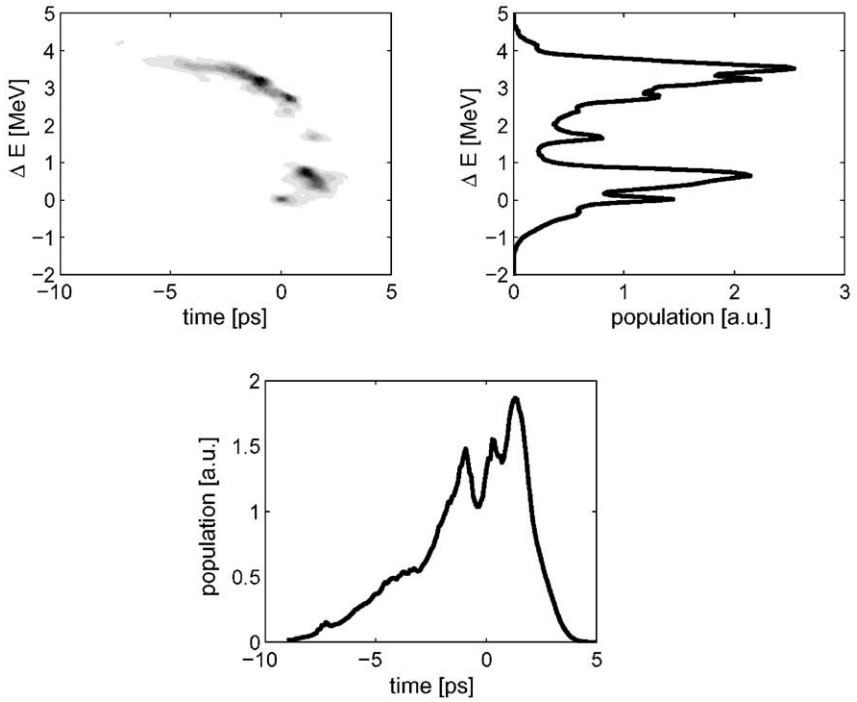


Fig. 4. Reconstructed longitudinal phase space downstream the bunch compressor (top left) and energy (top right) and time (bottom) charge density. (Time > 0 correspond to the bunch head).

FEL when the linac is operated so that the bunch compression is maximized. We discussed elsewhere [7] a possible mechanism, based on CSR self-interaction in the bunch compressor, that could account for our observation. In the TTF accelerator among the different source of wakefield that have been considered, CSR wakefield has the strength to yield an energy redistribution such as the one we have observed. Moreover, the CSR wake can be strongly enhanced due to local charge concentration, as pointed out in Ref. [8], e.g. due to longitudinal phase space curvature.

References

[1] Andruszkow, et al., Phys. Rev. Lett. 85 (2000) 3825.
[2] Ph. Piot, et al., Proceedings of EPAC 2000, Vienna, Austria, 2000, pp. 1546–1548.
[3] M. Borland, LEUTL-ANL, private communication, 2000.
[4] A. Kabel, et al., Proceedings of 1999 part. accel. conf., IEEE catalog #0-7803-5573-3/99, 1999, pp. 2507–2509.
[5] G. Minerbo, Comput. Graphics Image Process. 10 1970 48.
[6] M. Geitz, et al., Proceedings of the 1999 Part. Accel. Conference, IEEE Catalog #0-7803-5573-3/99, 1999, pp. 2174–2176.
[7] T. Limberg, Ph. Piot, E. Schneidmiller, An analysis of longitudinal phase space fragmentation at the TESLA test facility, Nucl. Instr. and Meth A 475 (2001) 353, these proceedings.
[8] R. Li, Proceedings of the EPAC 2000, Vienna, Austria, 2000, pp.1312–1314.